Bi-allelic Loss of Human *APC2*, Encoding Adenomatous Polyposis Coli Protein 2, Leads to Lissencephaly, Subcortical Heterotopia, and Global Developmental Delay

Sangmoon Lee,[1,2] Dillon Y. Chen,[1,2] Maha S. Zaki,[3] Reza Maroofian,[4,5] Henry Houlden,[5] Nataliya Di Donato,[6] Dalia Abdin,[6,7] Heba Morsy,[8] Ghayda M. Mirzaa,[9,10,11] William B. Dobyns,[9,10,12] Jennifer McEvoy-Venneri,[1] Valentina Stanley,[1] Kiely N. James,[1] Grazia M.S. Mancini,[13] Rachel Schot,[13] Tugba Kalayci,[13,14] Umut Altunoglu,[14] Ehsan Ghayoor Karimiani,[4] Lauren Brick,[15] Mariya Kozenko,[15] Yalda Jamshidi,[4] M. Chiara Manzini,[16] Mehran Beiraghi Toosi,[17] and Joseph G. Gleeson[1,2,*]

Lissencephaly is a severe brain malformation in which failure of neuronal migration results in agyria or pachygyria and in which the brain surface appears unusually smooth. It is often associated with microcephaly, profound intellectual disability, epilepsy, and impaired motor abilities. Twenty-two genes are associated with lissencephaly, accounting for approximately 80% of disease. Here we report on 12 individuals with a unique form of lissencephaly; these individuals come from eight unrelated families and have bi-allelic mutations in *APC2*, encoding adenomatous polyposis coli protein 2. Brain imaging studies demonstrate extensive posterior predominant lissencephaly, similar to *PAFAH1B1*-associated lissencephaly, as well as co-occurrence of subcortical heterotopia posterior to the caudate nuclei, "ribbon-like" heterotopia in the posterior frontal region, and dysplastic in-folding of the mesial occipital cortex. The established role of APC2 in integrating the actin and microtubule cytoskeletons to mediate cellular morphological changes suggests shared function with other lissencephaly-encoded cytoskeletal proteins such as α-N-catenin (CTNNA2) and platelet-activating factor acetylhydrolase 1b regulatory subunit 1 (PAFAH1B1, also known as LIS1). Our findings identify *APC2* as a radiographically distinguishable recessive form of lissencephaly.

The development of the cerebral cortex is a complex dynamic process that occurs primarily between gestational weeks 6 and 20. The predominant steps include neural stem cell proliferation and differentiation, migration from the ventricular site of origin outward to the developing cortical plate, and cortical organization associated with synaptogenesis and neural network formation. Disruption of this process can lead to many different malformations of cortical development (MCD), the diversity of which is increasingly highlighted through advances in both brain imaging and molecular genetics.[1] MCDs collectively represent a major cause of neurodevelopmental disorders; they are often associated with severe epilepsy and contribute to morbidity and mortality in the first decade of life.[2] MCDs associated with defects in neuronal migration include the lissencephaly spectrum of disorders (LIS, agyria-pachygyria) and less severe MCDs, including subcortical band heterotopia and tubulinopathy-associated dysgyrias.

Although some types of MCDs can result from environmental factors, those in the LIS spectrum are almost always due to recessive, dominant, or X-linked mutations, encoding proteins that regulate the neuronal cytoskeleton (both actin and microtubules)—a critical function as neurons migrate. To date, genes associated with these disorders include *ACTB* (MIM: 102630), *ACTG1* (MIM: 102560), *ARX* (MIM: 300382), *CDK5* (MIM: 123831), *CRADD* (MIM: 603454), *CTNNA2* (MIM: 114025), *DCX* (MIM: 300121), *DYNC1H1* (MIM: 600112), *KIF2A* (MIM: 602591), *KIF5C* (MIM: 604593), *PAFAH1B1* (also known as *LIS1*; MIM: 601545), *MACF1* (MIM: 608271), *MAST1* (MIM: 612256), *NDE1* (MIM: 609449), *RELN* (MIM: 600514), *TUBA1A* (MIM: 602529), *TUBB* (MIM: 191130), *TUBB2A* (MIM: 615101), *TUBB2B* (MIM: 612850), *TUBB3* (MIM: 602661), *TUBG1* (MIM: 191135), and *VLDLR* (MIM: 192977), and they account for more than 80% of individuals with LIS and LIS variants.[4,5] Differences in the gyral pattern and associated brain malformations, or other non-brain dysmorphisms, make it possible to distinguish some genetic forms of LIS. Some genes associate with a posterior-predominant (i.e., P > A) LIS (*PAFAH1B1*, *TUBA1A* and others), and others

[1]Department of Neurosciences, Howard Hughes Medical Institute, University of California, San Diego, CA 92093, USA; [2]Rady Children's Institute for Genomic Medicine, Rady Children's Hospital, San Diego, CA 92123, USA; [3]Clinical Genetics Department, Human Genetics and Genome Research Division, National Research Centre, Cairo 12311, Egypt; [4]Genetics Research Centre, Molecular and Clinical Sciences Institute, St. George's University, London SW17 0RE, UK; [5]Department of Neuromuscular Disorders, University College London Institute of Neurology, Queen Square, London WC1N 3BG, UK; [6]Institute for Clinical Genetics, Technische Universität Dresden, Fetscherstrasse 74, 01307 Dresden, Germany; [7]Human Cytogenetics Department, Human Genetics and Genome Research Division, National Research Centre, Cairo 12311, Egypt; [8]Human Genetics Department, Medical Research Institute, Alexandria University, Alexandria 21561, Egypt; [9]Center for Integrative Brain Research, Seattle Children's Research Institute, Seattle, WA 98101, USA; [10]Department of Pediatrics, University of Washington, Seattle Children's Research Institute, Seattle WA, 98101, USA; [11]Brotman Baty Institute for Precision Medicine, Seattle, WA 98195, USA; [12]Department of Neurology, University of Washington, Seattle Children's Research Institute, Seattle WA, 98101, USA; [13]Department of Clinical Genetics, Erasmus University Medical Center, 3015 CN Rotterdam, the Netherlands; [14]Department of Medical Genetics, Istanbul University, Istanbul Faculty of Medicine, Istanbul 34093, Turkey; [15]Department of Genetics, McMaster Children's Hospital, Hamilton, Ontario L8S 4L8, Canada; [16]Child Health Institute of New Jersey, Department of Neuroscience and Cell Biology, Rutgers Robert Wood Johnson Medical School, New Brunswick, NJ 08901, USA; [17]Department of Pediatric Neurology, Ghaem Hospital, Mashhad University of Medical Sciences, Mashhad 7HRJ+HQ, Iran
*Correspondence: jogleeson@ucsd.edu
https://doi.org/10.1016/j.ajhg.2019.08.013.

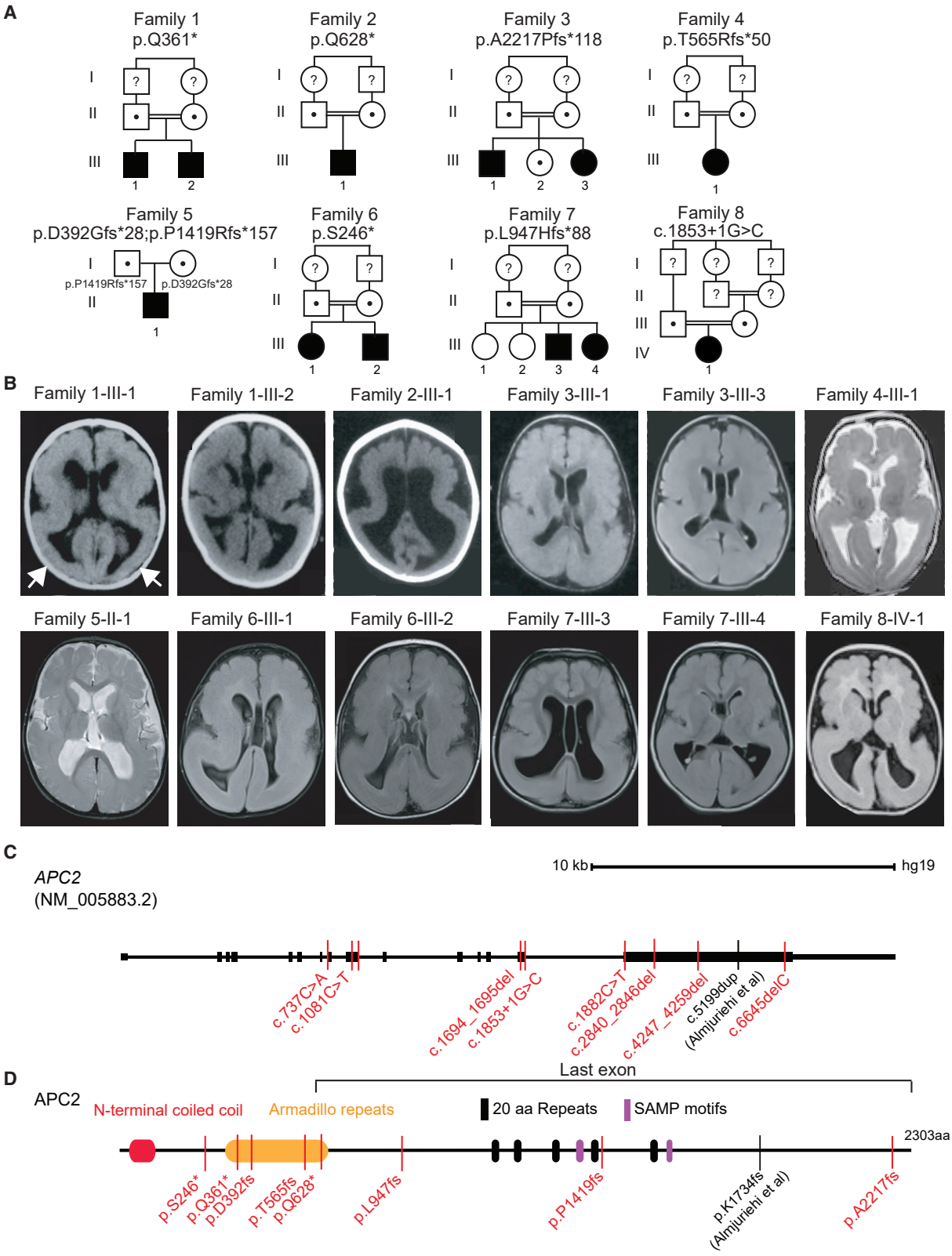

Figure 1. *APC2* Bi-allelic Loss of Function Mutations in Posterior-Predominant (P > A) Lissencephaly

(A) Twelve affected individuals from eight families showed unique bi-allelic mutations in *APC2*. All families except family 5 had documented parental consanguinity (double bars). The allele is listed below the family number. Dots and question marks indicate heterozygous carriers and samples not tested, respectively.

(B) Axial brain imaging in each family showed evidence of posterior-predominant lissencephaly. In families 1 and 2, only brain CT was available, but for other families, brain MRI is shown. Scans showed more severe agyria in the posterior than in the anterior cortex

(legend continued on next page)

with anterior-predominant (A > P) LIS (*DCX*, *ACTB*, *RELN* and others). The LIS gradient and associated brain and other malformations allow for distinction of at least 21 different subtypes of LIS and allow for prediction of likely mutant genes for newly identified individuals.[5]

In a collaborative effort to identify additional mechanisms underlying LIS, we recruited eight families for whom previous phenotypic and molecular analysis suggested a novel cause of the disorder. This cohort included families that could not be accurately classified into existing phenotypic categories or for whom testing for mutations in existing genes was negative. This study was performed within an ethical framework set by the University of California, San Diego IRB, and informed consent was obtained on each individual involved in this study. We recruited family 1 from Egypt; this family had documented parental 1st degree consanguinity and two affected male siblings who showed a nearly identical clinical pattern of severe developmental delay and myoclonic seizures starting at 5 months of age, along with a radiographic pattern of P > A LIS (Figures 1A and 1B). Genomic DNA from both affected individuals underwent whole-exome sequencing with the SureSelect Human All Exome 50 Mb kit (Agilent Technologies), and 125 bp paired-end read sequences were generated on a HiSeq2500 (Illumina), then analyzed according to GATK best practices (see Supplemental Methods). We identified a homozygous truncating p.Gln361* mutation in *APC2* (MIM: 612034) (GenBank: NM_005883.2, UCSC Genome Browser: uc002lsr.1) encoding adenomatous polyposis coli protein 2, which is expressed throughout the central nervous system.[6] Other homozygous variants in this family were relatively common, were less likely to damage protein function, or were already linked to other diseases; for example, *KCNMA1* (MIM 600150) loss causes autosomal-dominant paroxysmal nonkinesigenic dyskinesia (MIM: 609446), and *FBN1* (MIM: 134797) loss causes autosomal-dominant Marfan syndrome (MIM: 154700), which affected individuals do not have (Table S1).

Two other families from our lissencephaly cohort of 75 families with predominantly recessive MCDs also showed homozygous truncating mutations in *APC2*. Families 2 and 3 both had documented parental 1st degree consanguinity. Brain MRIs in both families showed a P > A LIS pattern that closely matched images of family 1. Family 2 had a single affected child and demonstrated a homozygous p.Gln628* mutation, whereas family 3 had two affected and one healthy child and demonstrated a homozygous p.Ala2217Profs*118 mutation in the affected individuals. These data suggest that homozygous loss of function (LoF) mutations in *APC2* lead to fully penetrant P > A LIS. Through Matchmaker Exchange and correspondence with colleagues, we identified five additional families in which there were truncating *APC2* mutations that were independently identified as likely to be most relevant to clinical presentation (Table S1) and in which brain MRIs of affected individuals showed P > A LIS. The protein alterations included homozygous p.Thr565Argfs*50, p.Ser246*, p.Leu947Hisfs*88 and c.1853+1G>C (splice donor), and compound heterozygous p.Asp392Glyfs*28;p.Pro1419Argfs*157. None of the eight families had damaging mutations in any known *LIS* genes. Thus, we identified a total of eight families that together included 12 individuals with bi-allelic *APC2* LoF mutations and P > A LIS, suggesting bi-allelic loss of *APC2* function as a rare cause of P > A LIS.

All affected children were born full term without any complications during pregnancy and delivery (Table 1). Although as a group length and weight at birth were normal, most affected individuals showed a trend toward smaller head circumference; only one individual met criteria for microcephaly, defined as a head size < 3 standard deviation (SD) below the mean, at the most recent measurement (Table 1). Most individuals presented at 3 months to 3 years of age with severe developmental delay, including absent or delayed milestones, and had seizures starting at 3 months to 5 years of age. Seizures were typically myoclonic or generalized tonic clonic and occurred daily to monthly. Electroencephalograms for most individuals showed generalized epileptiform activity. Neurological findings included hypotonia of the trunk and hypertonia of the extremities, along with alterations in deep tendon reflexes, features that are typical in severe LIS. None of the individuals were able to walk or had any language skills. Standard metabolic testing, visual evoked potentials, evaluation for dysmorphology, and review of organ systems were unremarkable in all tested individuals. Thus, clinical features do not distinguish *APC2*-LIS from the reported spectrum of typical severe LIS.

In five of the individuals, high-resolution brain MRIs were available for review (Figure 2), and these demonstrated features not common in other causes of LIS. All individuals demonstrated a P > A gradient, which has been reported with *PAFAH1B1, TUBG1, ARX, DYNC1H1* and can also be seen in association with *TUBA1A, TUBB2B, KIF5C*, and *KIF2A*.[5] In addition, ventriculomegaly with

(arrows in first scan highlight posterior agyria). Scans are T1 or FLAIR sequences, except for those of families 4 and 5, which are T2 sequences.
(C) Gene organization of *APC2*. The scale bar represents 10 kb. *APC2* contains 15 exons, the first of which is non-coding. Mutations were scattered throughout the coding region of the protein; five mutations were present in large exon 15. Exon 15 also contains the homozygous c.5199dup Almuriekhi et al. mutation.[16]
(D) APC2 is a 2,303 amino acid multidomain scaffolding protein containing an N-terminal coiled-coil, Armadillo repeats, 20 amino acid (aa) repeats (FXVEXTPXCFSRXSSLSSLS), and SAMP (Ser-Ala-Met-Pro) motifs. Affected individuals' mutations, represented with simplified nomenclature, were located throughout the open reading frame. The region of the protein encoded by the last exon is highlighted.

Table 1. Clinical Features of Individuals with *APC2* Mutations

	Family 1		Family 2	Family 3		Family 4	Family 5	Family 6		Family 7		Family 8
Origin	Egypt		Egypt	Egypt		Iran	USA	Turkey		Syria		Egypt
Variant												
Zygosity	homozygous		homozygous	homozygous		homozygous	compound heterozygous	homozygous		homozygous		homozygous
Genomic (hg19)	chr19: g.1457116C>T		chr19: g.1465182C>T	chr19: g.1469945delC		chr19: g.1462017_1462018delCA	chr19: g.1457202del; g.1467547del	chr19: g.1456324C>A		chr19 :g.1466140_1466146del		chr19: g.1462177G>C
cDNA	c.1081C>T		c.1882C>T	c.6645delC		c.1694_1695delCA	c.1167_1180del; c.4247_4259del	c.737C>A		c.2840_2846del		c.1853+1G>C
Protein	p.Gln361*		p.Gln628*	p.A2217fs*118		p.T565Rfs*50	p.D392Gfs*; p.P1419Rfs*157	p.Ser246*		p.L947Hfs*88		Splice donor
Proband	**1-III-1**	**1-III-2**	**2-III-1**	**3-III-1**	**3-III-3**	**4-III-1**	**5-II-1**	**6-III-1**	**6-III-2**	**7-III-3**	**7-III-4**	**8-IV-1**
Gender	M	M	M	M	F	F	M	F	M	M	F	F
Weight at birth (kg)	3.2 (−0.5 SD)	3 (−1 SD)	3.5 (mean)	3 (−1 SD)	3.2 (−0.3 SD)	3.9 (mean)	10–25 centiles	2.9 (−1.0 SD)	3 (−0.9 SD)	∼2	∼2	NA (normal)
Length at birth (cm)	50 (mean)	49 (−0.2 SD)	49 (−0.2 SD)	50 mean	48 (−0.2 SD)	50 (mean)	10–25 centiles	48 (−0.7 SD)	49 (−0.5 SD)	NA	NA	NA (normal)
HC at birth (cm)	35 (−0.5 SD)	34.5 (−0.8 SD)	34.5 (−0.8 SD)	35 (−0.5 SD)	34 (−0.8 SD)	37 (mean)	90–95 centiles	34 (−0.4 SD)	34 (−0.6 SD)	NA	NA	NA (normal)
Age at last examination	2 years	9 months	2 years	15 years	5 years	3 years	7.5 years	4 years	2 years	4 years, 7 months	6 years	7 months
HC at last examination (cm)	48.5 (−0.1 SD)	43.5 (−1.4SD)	49 (mean)	51 (−2.6SD)	48.5 (−1.3SD)	45 (−3.8 SD)	NA	47 (−2.1SD)	44.5 (−3.1SD)	47 (−2.9 SD)	47 (−SD)	NA
Diagnosis age	3 years	3 months	2 years	2 years	6 months	3 months	19 months	18 months	8 months	6 months	4 months	7 months
Intellectual Disability	severe	severe	severe	severe	severe	severe	severe	severe	severe	severe	severe	severe
Psychomotor Development												
Gross motor	delayed	delayed	delayed	delayed	delayed	delayed	delayed	delayed	delayed	delayed	delayed	delayed, no head control
Fine motor	absent	absent	absent	absent	absent	absent	delayed	delayed	delayed	delayed	delayed	delayed
Language	delayed	delayed	delayed	absent	absent	delayed	delayed	delayed	delayed	absent	absent	NA

(*Continued on next page*)

Table 1. ***Continued***

	Family 1		**Family 2**	**Family 3**		**Family 4**	**Family 5**	**Family 6**		**Family 7**		**Family 8**
Social	delayed	delayed	delayed	delayed	delayed	delayed	unknown	delayed	delayed	delayed	delayed	delayed
Seizures	**Y**	**Y**	**Y**	**Y**	**Y**	**N**	**N**	**Y**	**Y**	**Y**	**N**	**N**
Age of Onset	5 months	3 months	4 months	6 years	4.5 years	–	–	12 months	18 months	2 years	–	–
Type	generalized and myoclonic	generalized and myoclonic	myoclonic seizure and infantile spasm	generalized and myoclonic	generalized and myoclonic	–	–	generalized and myoclonic	generalized and myoclonic	generalized and myoclonic	–	–
Frequency	monthly	monthly	daily	with fever	daily	–	–	daily	daily	weekly	–	–
Controlled/ Refractory	fairly controlled	fairly controlled	refractory	controlled	refractory	–	–	refractory	refractory	controlled	–	–
EEG	generalized epileptogenic activity involving midline structure	generalized epileptogenic activity	hypsarrhythmia	bilateral tempro-pariental epileptogenic activity	generalized epileptoggenic activity	normal	normal	generalized epileptogenic activity	generalized epileptogenic activity	NA	NA	NA
Neurological Findings												
Hypertonia	Y	Y	N	N	N	N	N	N	N	Y, peripheral	Y, peripheral	N
Hypotonia	N	N	Y	Y	Y	Y, truncal	Y	Y	Y	Y, central	Y, central	Y
Spastic tetraplegia	Y	Y	tetraplegia but not spastic	N	N	spastic dystonia	NA	N	N	Y	N	N
Investigations												
Metabolic	normal	normal	normal	normal	normal	normal	NA	normal	normal	normal	normal	NA
VEP and ERG	normal	normal	normal	normal	normal	normal	NA	NA	NA	NA	NA	NA
Neuroimaging	**CT**	**CT**	**CT**	**MRI**	**MRI**	**MRI**	**MRI**	**MRI**	**MRI**	**MRI**	**MRI**	**MRI**
P > A Lissencephaly	Y	Y	Y	Y	Y	Y	Y	Y	Y	Y	Y	Y
Cerebral mantle thickening	>1 cm	>1 cm	unknown	>1 cm	>1 cm	8–10 mm	NA	Y	Y	Y	Y	>1 cm
Ribbon heterotopia	NA	NA	NA	N	N	N	Y	Y	Y	Y	Y	N
Corpus callosum hypogenesis	Y	Y	Y	Y	N	Y	Y	Y	Y	Y	Y	Y
Cerebellar hypoplasia	N	N	N	N	N	very mild	N	very mild	N	N	N	N

(*Continued on next page*)

Table 1. *Continued*

	Family 1		Family 2	Family 3		Family 4	Family 5	Family 6		Family 7		Family 8
Brainstem hypoplasia	N	N	N	N	N	N	N	very mild	Y	small pons	small pons	N
Ventriculomegly	Y	Y	Y	Y	Y	Y	Y	Y	Y	Y	Y	mild
White matter paucity	Y	Y	Y	Y	Y	Y	Y	Y	Y	Y	Y	Y

Genomic position of allele is presented in hg19 reference. Abbreviations are as follows: cm, centimeter; F, female; M, male; HC, head circumference; L, left; MRI, magnetic resonance imaging; NA, not available; –, negative; R, right; SD, standard deviation; VEP, visual evoked potential; and ERG, electroretinogram.

stretched and thinned corpus callosum and an unusual posterior subcortical heterotopia just posterior to the caudate nuclei were noted in several individuals. In some individuals, the subcortical heterotopia appeared to merge with the deep cellular layer of the posterior agyria, and almost no white matter was visible. One child (6-III-2) had an undulating, ribbon-like deep cellular layer (Figure 2L) that began in the mid-frontal lobe and continued posteriorly to the parietal lobe, in a pattern that was very different from the subcortical band heterotopia (MIM: 300067) seen with *DCX* mutations. The ribbon-shaped subcortical heterotopia of subject 6-III-2 was reminiscent of the ribbon-like heterotopia observed with *EML1* mutations (MIM: 600348).[7] However, *EML1* mutations are also associated with hydrocephalus, agenesis of the corpus callosum, and diffuse polymicrogyria. Additionally, with *CENPJ* mutation (MIM: 608393), a more discrete thin festooned heterotopia in the areas lateral and adjacent to the striatum has been seen (W.B.D. personal observation), and thin subcortical heterotopia band in the upper frontal area and parallel to the lateral ventricles is reported with *GPSM2* mutations causing Chudley-McCullough syndrome (MIM: 604213).[8] However, the pattern of subcortical heterotopia seen in these conditions is different from that of *APC2*. In addition, all subjects showed hippocampal defects (Figure S1) and striking dysplastic infolding of the mesial occipital cortex, neither of which are seen in other forms of LIS (Figure 2; examples can be seen in Figures 2B, 2F, 2J, 2N, and 2R). In fact, recognizable brain MRI findings (W.B.D., unpublished data) ultimately led to the clinical diagnosis of the affected individual from family 8 as most likely harboring *APC2*. Thus, we believe that the images can distinguish *APC2*-LIS from other forms of disease.

The adenomatous polyposis coli gene family (not to be confused with the multisubunit anaphase promoting complex) consists of two paralogs conserved to *Drosophila*, *APC* (MIM: 611730) and *APC2*. *APC* was first identified as a human colon cancer tumor suppressor, associated with both sporadic and inherited forms of the disease,[9] and APC functions as a negative regulator of Wnt signaling and in the organization and regulation of the actin and microtubule cytoskeletons.[10] APC2 (also called APCL) is highly similar to APC in its N-terminal armadillo-repeat containing half, but it shares little sequence similarity to its C-terminal half. APC2 is not mutated in colon cancer, binds less efficiently to β-catenin than APC, and has not been implicated in Wnt signaling.[11,12] APC2 localizes to actin and microtubule fibers, and $Apc2^{-/-}$ mice show disrupted neuronal migration, leading to defects in lamination of the cerebral cortex and cerebellum[13] and thus supporting *APC2* as a LIS candidate gene.

Encoded on human chromosome 19, *APC2* consists of 15 coding exons and a 10.1 kb coding mRNA. Three alternative splice isoforms are described, but the major isoform encodes a 2,303 amino acid protein. We identified truncating mutations in four of these exons, and we found

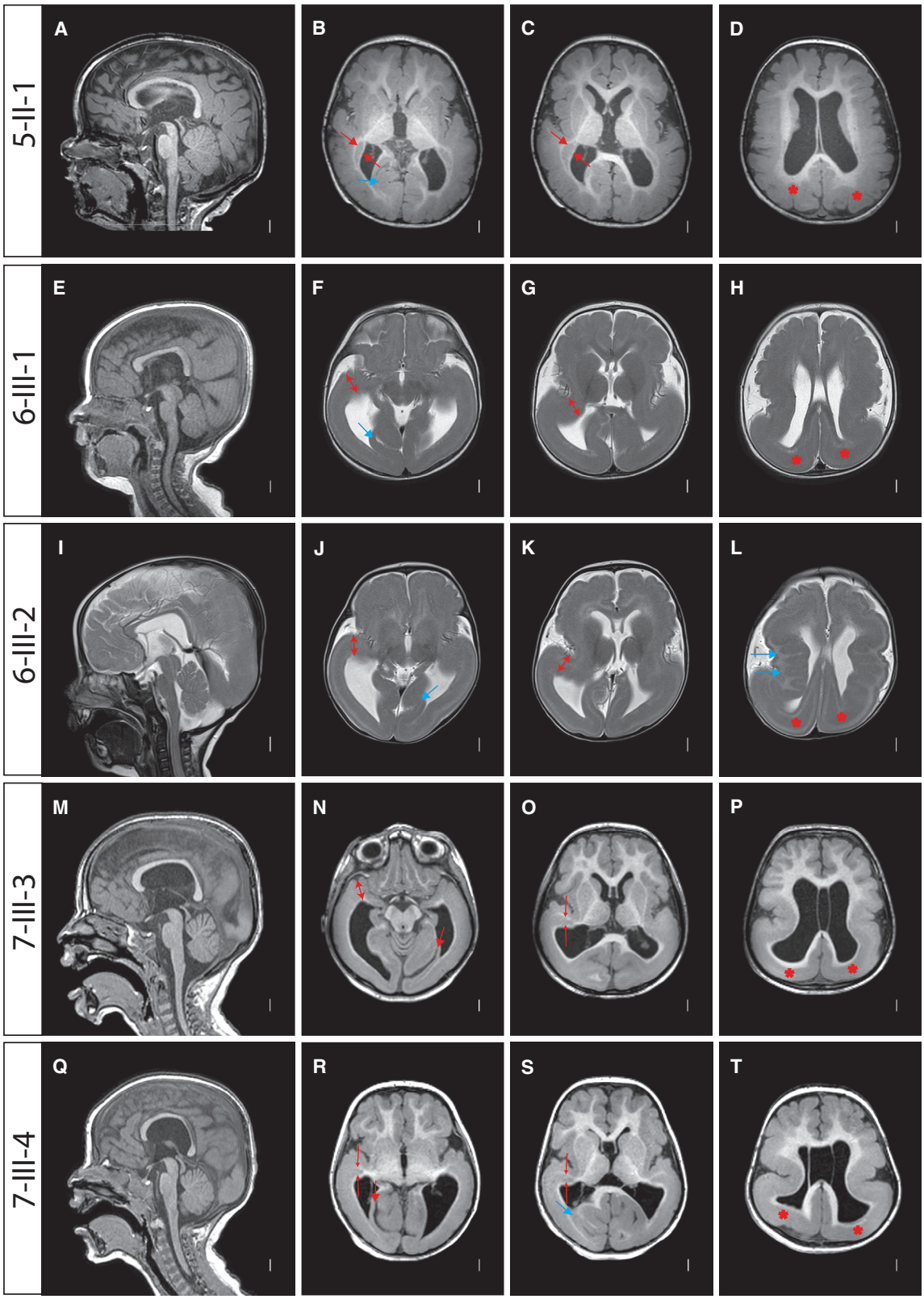

Figure 2. Posterior-Predominant (P > A) LIS with Subcortical Ribbon Heterotopia Associated with Bi-allelic *APC2* Mutations
Individual identifier along left. Midline sagittal MRIs showed P > A LIS with a stretched and thinned corpus callosum and relatively well-preserved anterior folding, brainstem, and cerebellar architecture. Axial images all showed P > A LIS with mild (B–D, N–P, and R–T) or moderate (F–H and J–L) frontal pachygyria and posterior agyria (asterisks shown in fourth column only). 5-II-1: short, comma-shaped subcortical heterotopias began just posterior to and at the same level as the tail of the caudate nuclei (between the red arrows in [B and C]). 7-III-3 and 7-III-4: same subcortical heterotopia began in the same place, but then merged with the deep cellular layer of the posterior

(legend continued on next page)

that most occurred in the largest and last exon, exon 15 (Figure 1C). The four truncating mutations identified in the last exon were predicted to lead to a stable mRNA and potentially a C-terminally truncated protein, whereas mutations in earlier exons were predicted to lead to nonsense mediated decay and LoF. We considered the possibility that late truncating mutations might have a milder phenotype than early truncating mutations, but we found no evidence of milder clinical or radiographic phenotypes. The locations of the truncating mutations occurred throughout the open reading frame (Figure 1D), and the lack of correlation of the location with the severity of the imaging phenotype suggested that most or all of these mutations are LoF. The variants were unique in our dataset of >5,000 exomes from individuals with neurodevelopmental phenotypes and were not represented in the Greater Middle Eastern Variome, 1000 Genomes, or gnomAD databases (Table S1). All variants were confirmed by Sanger sequencing and segregated according to a recessive mode of inheritance.

APC2 has pLI value of 1.0 in gnomAD, suggesting haploinsufficiency intolerance. However, heterozygous carriers in this study did not have any noticeable phenotype. Constraint metrics such as pLI and the more recently introduced o/e ratio represent a spectrum of tolerance to inactivation.[14] Although pLI is generally accepted as an indicator of LoF intolerance, not all genes with a high pLI score cause disease, even if they have heterozygous LoF variants. Thus, a pLI of 1.0 of *APC2* does not necessarily mean that heterozygous LoF variants of *APC2* cause haploinsufficiency or disease. In fact, 27 heterozygous *APC2* variants that have been predicted to be LoF with high confidence were found in gnomAD in apparently healthy individuals. This means that heterozygous LoF variants of *APC2* are probably not sufficient to produce disease, might produce disease in specific genetic backgrounds, or might be subject to purifying selection on the population rather than the individual level.[15] Therefore, heterozygous carriers in our study might have an unnoticeable phenotype, although they were not examined by brain MRI.

A recent publication identified a late truncating homozygous single-base duplication (p.Lys1734Glnfs*419; Figures 1C and 1D) in exon 15 of *APC2* in two affected children from a consanguineous marriage. These children displayed Sotos-like features but had no noted brain malformations (MIM: 617169).[16] Sotos syndrome is a form of cerebral gigantism and is associated with intellectual disability and macrocephaly (MIM: 117550). The children showed developmental delay and macrocephaly, and brain MRIs showed only dilated brain ventricles. We reviewed the brain MRIs in the published paper and found no evidence of LIS. The reported variant was predicted to lead to replacement of the C-terminal 570 amino acids with 418 aberrant residues. Despite the fact that all of our affected individuals had bi-allelic truncating mutations throughout the protein, none of our subjects showed macrocephaly or Sotos-like features. This leaves the open question as to why this reported homozygous frameshift variant did not produce LIS. Possibilities include (1) that the variant did not fully inactivate the protein, (2) that it produced a novel function, and (3) that it is an allele-specific association.[17] Determining the full phenotypic spectrum associated with *APC2* mutations as additional individuals and alleles are identified will require further work.

The role of APC2 in LIS remains to be established, but the phenotypes we report together with APC2's published localization and binding partners support functional interaction with other LIS-related proteins. In migratory neurons, APC2 partially co-localizes with microtubules and F-actin at the leading edge of the growth cone.[13] In *Apc2*$^{-/-}$ neurons, BDNF stimulation fails to increase the amount of F-actin at the leading edge or effectively stabilize microtubules.

We recently reported on homozygous *CTNNA2* mutations in LIS, and like APC2, the *CTNNA2*-encoded protein (α-N-catenin) can interact with both β-catenin and actin. In *CTNNA2*-related LIS, defects in Wnt signaling were excluded; instead, α-N-catenin competed with the Arp2/3 complex to suppress actin branching,[18] leading to more stable leading neurites. Another recent report linked APC to cytoplasmic dynein through the cofactor AMER (APC-membrane recruitment) family of membrane-bound proteins.[19] Furthermore, APC has been reported to play an important role in regulation of radial glial polarity and interneuron migration by modulating microtubule severing and to be essential for cortex development.[20,21] APC2 might similarly serve as a microtubule regulator or form a complex with α-N-catenin or dynein to mediate neurite stability or the minus-end-directed dynein forces required during migration, although further experimental studies should follow to support these speculations. Interestingly, a genetic interaction between *Pafah1b1* and *Apc* in murine neuronal migration was reported, but investigations of *Apc2* were not performed.[22] Finally, in postmitotic neurons, APC2 controls dendritic development by promoting microtubule dynamics through two separate microtubule binding domains.[23] It is possible that these domains function during neuronal migration to mediate leading-process organization.

agyria (thin red arrows in O, R, and S). 6-III-1 and 6-III-2 (and in [R]): this same region appeared to have dysplastic cortex extending from the pial surface to the ventricular surface, with no white matter apparent (two-headed arrows in [F], [G], [J], [K], and [N]). The ribbon heterotopia began at this level (two-headed arrow in [K]). All subjects showed striking dysplastic in-folding of one or several gyri in the mesial occipital region (thick blue or red arrows in all five images in second column). The selected images include T1-weighted (A–D and M–T) and T2-weighted (E–L) images in the midline sagittal (first column) and multiple axial planes progressed from low to high slices (second to fourth columns).

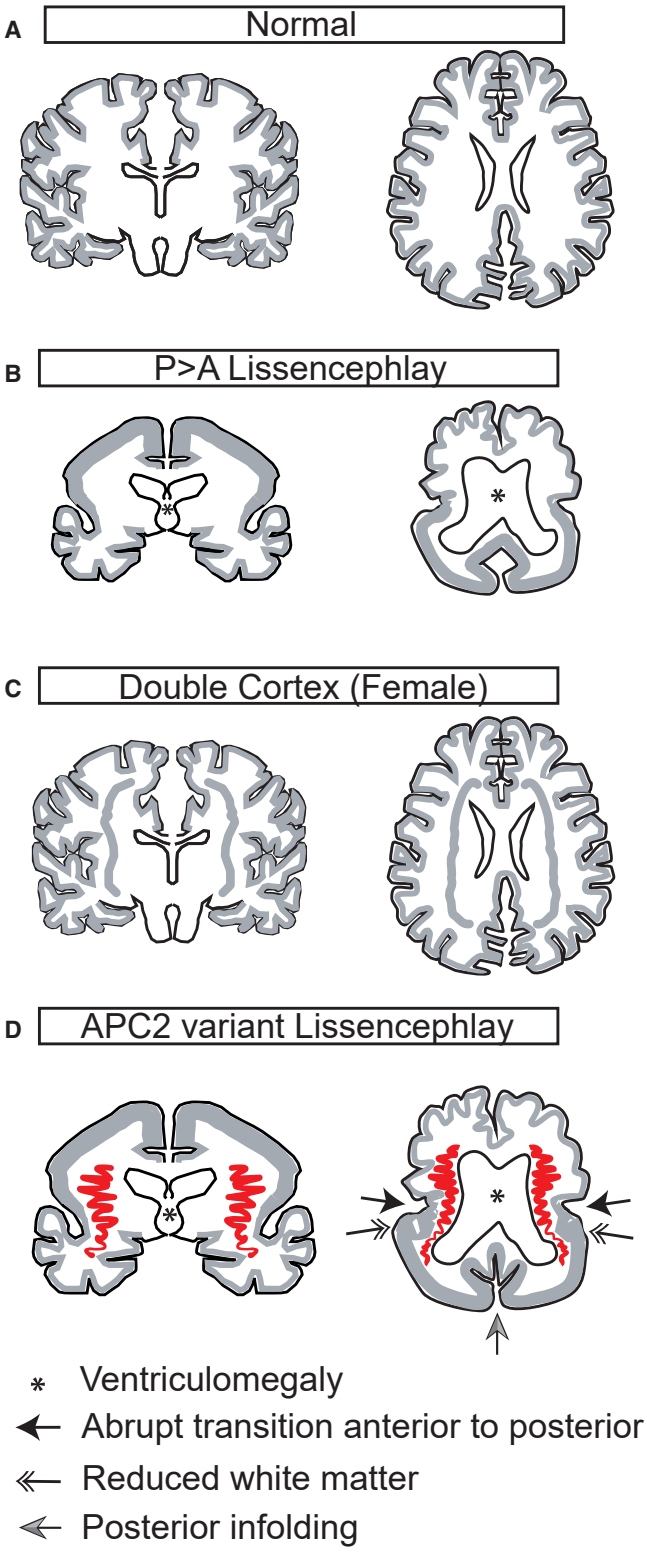

Figure 3. Schematic Depiction of Major Migrational Defects in Lissencephaly Subtypes

(A) The normal type shows evenly spaced cortical gyri and sulci and a thin mantle of gray matter.

(B) The P > A lissencephaly subtype shows thickened cortical gray matter mantle in the neocortex (left); this gray matter is more severe in the posterior cortex (right). Ventriculomegaly is also depicted (*).

(C) The double-cortex subtype shows a normally gyrated outer cortex with a normal cortical mantle, but additionally it shows a band heterotopia, which is evenly distributed anteriorly and posteriorly in the subcortical white matter.

(D) *APC2* lissencephaly shows P > A gradient with a thickened cortical gray matter mantle in the posterior and relatively preserved gyration in the anterior; the transition is abrupt (arrow). In the temporal region, the dysplastic cortex extends from the pia to the ventricle, resulting in reduced white matter (double arrow). Ribbon-like heterotopia is most noticeable in the perisylvian region and appears to connect with the tail of the caudate nuclei (red). In-folding of cortex in the mesial occipital region is often apparent (gray arrow).

In summary, we implicate *APC2* in a recessive form of P > A LIS, clinically characterized by severe intellectual disability, epilepsy, and neuromotor involvement and radiographically characterized by a stretched and thinned corpus callosum, subcortical thin and sometimes ribbon-shaped heterotopia in posterior perisylvian areas, and dysplastic in-folding of gyri in the mesial occipital cortex (Figure 3). There are most likely a range of developmental brain phenotypes resulting from loss of *APC2*, although our subjects are likely to be at the most severe end of the spectrum given the nature of the alleles. Elucidating the full range of phenotypes, genotype-phenotype correlations, and mechanisms of pathogenicity will require future studies.

Supplemental Data

Supplemental Data can be found online at https://doi.org/10.1016/j.ajhg.2019.08.013.

Acknowledgments

We thank the children and their families for their contributions to this study. This work was supported by National Institutes of Health grants U01 MH108898, R01 NS048453, R01 NS098004, the Simons Foundation Autism Research Initiative (SFARI), the Howard Hughes Medical Institute (J.G.G.), Qatar National Research Foundation 6-1463 (J.G.G.), and the March of Dimes 6-FY14-422 (M.C.M.). G.M.S.M. is supported by the ZonMW TOP grant 91217045. N.D.D., U.A., W.B.D., G.M.M., G.M.S.M., and M.S.Z. are members of the European Network on Brain Malformations (Neuro-MIG, European Cooperation in Science and Technology [COST] Action CA16118). T.K. was supported by COST Action CA16118 (STSM grant #41344). G.M.M. is supported by National Institutes of Health grant K08NS092898 and Jordan's Guardian Angels. Data on one family was collected as part of the SYNaPS Study Group collaboration funded by The Wellcome Trust and strategic award (Synaptopathies) funding (WT093205 MA and WT104033AIA). This research was conducted as part of the University College London Queen Square Genomics group, supported by the National Institute for Health Research University College London Hospitals Biomedical Research Centre. We thank the Rady Children's Institute for Genomic Medicine, the Broad Institute (U54HG003067 to E. Lander and UM1HG008900 to D. MacArthur), the Yale Center for Mendelian Disorders (U54HG006504 to R. Lifton and Murat Gunel) for sequencing support, and the Matchmaker Exchange. We acknowledge M. Gerstein, S. Mane, A.B. Ekici, S. Uebe, E.S. Cauley, and the University of California, San Diego Institute for Genomic Medicine Genetics Center for sequencing support and analysis, the Yale Biomedical High-Performance Computing Center

for data analysis and storage, the Yale Program on Neurogenetics, and the Yale Center for Human Genetics.

Declaration of Interests

The authors declare no competing interests.

Received: May 30, 2019
Accepted: August 28, 2019
Published: October 3, 2019

Web Resources

1000 Genomes http://www.1000genomes.org/
dbSNP http://www.ncbi.nlm.nih.gov/SNP/
GenBank http://www.ncbi.nlm.nih.gov/genbank/
GeneReviews, Bahi-Buisson, N., and Cavallin, M. (1993). Tubulinopathies Overview. https://www.ncbi.nlm.nih.gov/books/NBK350554/
Greater Middle East Variome Project, http://igm.ucsd.edu/gme/
gnomAD https://gnomad.broadinstitute.org/
Matchmaker Exchange https://www.matchmakerexchange.org/
OMIM http://www.omim.org/
UniProt http://www.uniprot.org/uniprot/
VEP https://www.ensembl.org/vep

References

1. Guerrini, R., Dobyns, W.B., and Barkovich, A.J. (2008). Abnormal development of the human cerebral cortex: genetics, functional consequences and treatment options. Trends Neurosci. *31*, 154–162.
2. Parrini, E., Conti, V., Dobyns, W.B., and Guerrini, R. (2016). Genetic basis of brain malformations. Mol. Syndromol. *7*, 220–233.
4. Di Donato, N., Kuechler, A., Vergano, S., Heinritz, W., Bodurtha, J., Merchant, S.R., Breningstall, G., Ladda, R., Sell, S., Altmüller, J., et al. (2016). Update on the ACTG1-associated Baraitser-Winter cerebrofrontofacial syndrome. Am. J. Med. Genet. A. *170*, 2644–2651.
5. Di Donato, N., Timms, A.E., Aldinger, K.A., Mirzaa, G.M., Bennett, J.T., Collins, S., Olds, C., Mei, D., Chiari, S., Carvill, G., et al. (2018). Analysis of 17 genes detects mutations in 81% of 811 patients with lissencephaly. Genet. Med. *20*, 1354–1364.
6. van Es, J.H., Kirkpatrick, C., van de Wetering, M., Molenaar, M., Miles, A., Kuipers, J., Destrée, O., Peifer, M., and Clevers, H. (1999). Identification of APC2, a homologue of the adenomatous polyposis coli tumour suppressor. Curr. Biol. *9*, 105–108.
7. Kielar, M., Tuy, F.P., Bizzotto, S., Lebrand, C., de Juan Romero, C., Poirier, K., Oegema, R., Mancini, G.M., Bahi-Buisson, N., Olaso, R., et al. (2014). Mutations in Eml1 lead to ectopic progenitors and neuronal heterotopia in mouse and human. Nat. Neurosci. *17*, 923–933.
8. Kau, T., Veraguth, D., Schiegl, H., Scheer, I., and Boltshauser, E. (2012). Chudley-McCullough syndrome: case report and review of the neuroimaging spectrum. Neuropediatrics *43*, 44–47.
9. Groden, J., Thliveris, A., Samowitz, W., Carlson, M., Gelbert, L., Albertsen, H., Joslyn, G., Stevens, J., Spirio, L., Robertson, M., et al. (1991). Identification and characterization of the familial adenomatous polyposis coli gene. Cell *66*, 589–600.
10. Aoki, K., and Taketo, M.M. (2007). Adenomatous polyposis coli (APC): A multi-functional tumor suppressor gene. J. Cell Sci. *120*, 3327–3335.
11. Schneikert, J., Vijaya Chandra, S.H., Ruppert, J.G., Ray, S., Wenzel, E.M., and Behrens, J. (2013). Functional comparison of human adenomatous polyposis coli (APC) and APC-like in targeting beta-catenin for degradation. PLoS ONE *8*, e68072.
12. Zhou, M.N., Kunttas-Tatli, E., Zimmerman, S., Zhouzheng, F., and McCartney, B.M. (2011). Cortical localization of APC2 plays a role in actin organization but not in Wnt signaling in *Drosophila*. J. Cell Sci. *124*, 1589–1600.
13. Shintani, T., Takeuchi, Y., Fujikawa, A., and Noda, M. (2012). Directional neuronal migration is impaired in mice lacking adenomatous polyposis coli 2. J. Neurosci. *32*, 6468–6484.
14. Karczewski, K.J., Francioli, L.C., Tiao, G., Cummings, B.B., Alföldi, J., Wang, Q., Collins, R.L., Laricchia, K.M., Ganna, A., and Birnbaum, D.P. (2019). Variation across 141,456 human exomes and genomes reveals the spectrum of loss-of-function intolerance across human protein-coding genes. bioRxiv. https://doi.org/10.1101/531210.
15. Cassa, C.A., Weghorn, D., Balick, D.J., Jordan, D.M., Nusinow, D., Samocha, K.E., O'Donnell-Luria, A., MacArthur, D.G., Daly, M.J., Beier, D.R., and Sunyaev, S.R. (2017). Estimating the selective effects of heterozygous protein-truncating variants from human exome data. Nat. Genet. *49*, 806–810.
16. Almuriekhi, M., Shintani, T., Fahiminiya, S., Fujikawa, A., Kuboyama, K., Takeuchi, Y., Nawaz, Z., Nadaf, J., Kamel, H., Kitam, A.K., et al. (2015). Loss-of-function mutation in APC2 causes Sotos syndrome features. Cell Rep. *10*, 1585–1598.
17. De Franco, E., Watson, R.A., Weninger, W.J., Wong, C.C., Flanagan, S.E., Caswell, R., Green, A., Tudor, C., Lelliott, C.J., Geyer, S.H., et al. (2019). A specific CNOT1 mutation results in a novel syndrome of pancreatic agenesis and holoprosencephaly through impaired pancreatic and neurological development. Am. J. Hum. Genet. *104*, 985–989.
18. Schaffer, A.E., Breuss, M.W., Caglayan, A.O., Al-Sanaa, N., Al-Abdulwahed, H.Y., Kaymakçalan, H., Yılmaz, C., Zaki, M.S., Rosti, R.O., Copeland, B., et al. (2018). Biallelic loss of human CTNNA2, encoding αN-catenin, leads to ARP2/3 complex overactivity and disordered cortical neuronal migration. Nat. Genet. *50*, 1093–1101.
19. Gao, F.J., Shi, L., Hines, T., Hebbar, S., Neufeld, K.L., and Smith, D.S. (2017). Insulin signaling regulates a functional interaction between adenomatous polyposis coli and cytoplasmic dynein. Mol. Biol. Cell *28*, 587–599.
20. Yokota, Y., Kim, W.Y., Chen, Y., Wang, X., Stanco, A., Komuro, Y., Snider, W., and Anton, E.S. (2009). The adenomatous polyposis coli protein is an essential regulator of radial glial polarity and construction of the cerebral cortex. Neuron *61*, 42–56.
21. Eom, T.Y., Stanco, A., Guo, J., Wilkins, G., Deslauriers, D., Yan, J., Monckton, C., Blair, J., Oon, E., Perez, A., et al. (2014). Differential regulation of microtubule severing by APC underlies distinct patterns of projection neuron and interneuron migration. Dev. Cell *31*, 677–689.
22. Hebbar, S., Guillotte, A.M., Mesngon, M.T., Zhou, Q., Wynshaw-Boris, A., and Smith, D.S. (2008). Genetic enhancement of the Lis1+/- phenotype by a heterozygous mutation in the adenomatous polyposis coli gene. Dev. Neurosci. *30*, 157–170.
23. Kahn, O.I., Schätzle, P., van de Willige, D., Tas, R.P., Lindhout, F.W., Portegies, S., Kapitein, L.C., and Hoogenraad, C.C. (2018). APC2 controls dendrite development by promoting microtubule dynamics. Nat. Commun. *9*, 2773.

The American Journal of Human Genetics, Volume *105*

Supplemental Data

Bi-allelic Loss of Human *APC2*, Encoding Adenomatous Polyposis Coli Protein 2, Leads to Lissencephaly, Subcortical Heterotopia, and Global Developmental Delay

Sangmoon Lee, Dillon Y. Chen, Maha S. Zaki, Reza Maroofian, Henry Houlden, Nataliya Di Donato, Dalia Abdin, Heba Morsy, Ghayda M. Mirzaa, William B. Dobyns, Jennifer McEvoy-Venneri, Valentina Stanley, Kiely N. James, Grazia M.S. Mancini, Rachel Schot, Tugba Kalayci, Umut Altunoglu, Ehsan Ghayoor Karimiani, Lauren Brick, Mariya Kozenko, Yalda Jamshidi, M. Chiara Manzini, Mehran Beiraghi Toosi, and Joseph G. Gleeson

Supplemental Figures

Figure S1

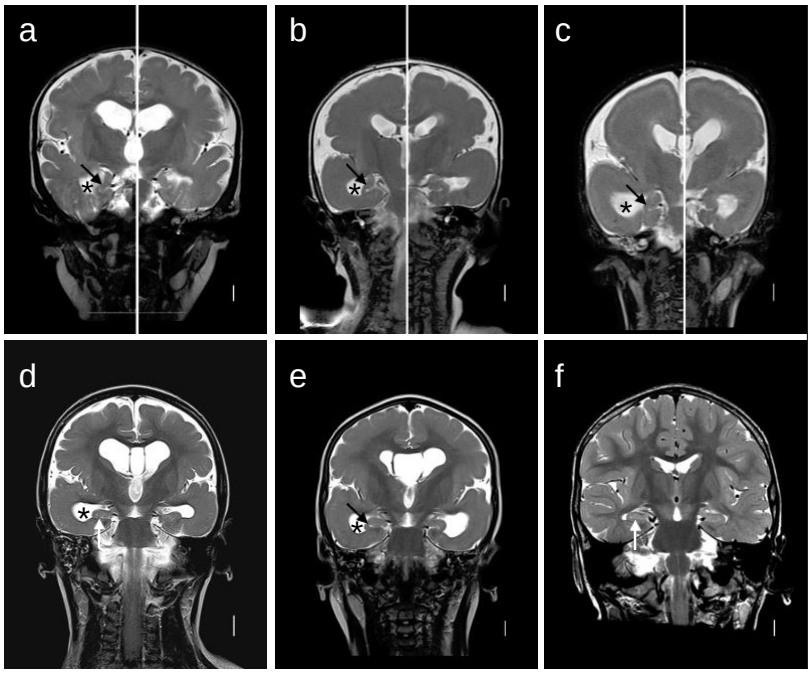

Figure S1. Brain imaging in *APC2*-lissencephaly in 5 children highlighting hippocampal malformations. Subjects 5-II-1 (**a**), 6-III-1 (**b**), 6-III-2 (**c**), 7-III-3 (**d**), 7-III-4 (**e**), and a normal control (**f**). The T2-weighted coronal images through the posterior frontal lobes and hippocampi showed globular and open hippocampi (**a-c**, **e**) that were usually under developed (**a-c**). The hippocampi in one child appear normal on these images (**d**), but all five subjects have moderately enlarged temporal horns (asterisks in **a-e**), which is commonly seen with hippocampal malformations associated with lissencephaly. All images are T2-weighted.

Supplemental Table

Table S1

	Gene	Zygosity	Chr	Pos	Ref	Alt	cDNA	AAChange	Segregated	OMIM	Effect	Impact	Transcript	dbSNP	gnomAD_AF	SIFT	PolyPhen	CADD_PHRED	Associated recessive disease
Family 1	VSTM4	hom	10	50272764	T	C	c.652A>G	p.(Lys218Glu)			missense_variant	MODERATE	NM_001031746.4		0.000012	deleterious(0)	probably_damagi	24.1	
	KCNMA1	hom	10	78651483	G	A	c.2986-6C>T	p.?		600150	splice_region_var	MODERATE	NM_001014797.2	201087232	0.000008	-	-	-	
	TGM7	hom	15	43584295	T	A	c.440A>T	p.(Glu147Val)		606776	missense_variant	MODERATE	NM_052955.2	181416302	0.000060	deleterious(0.01)	probably_damagi	26.5	
	FBN1	hom	15	48758054	G	A	c.4749C>T	p.(Ser1583=)		134797	splice_region_var	MODERATE	NM_000138.4		-	-	-	12.02	
	WDR18	hom	19	989769	C	T	c.329C>T	p.(Thr110Ile)	Y		missense_variant	MODERATE	NM_024100.3		-	deleterious(0.04)	probably_damagi	25.4	
	APC2	hom	19	1457116	C	T	c.1081C>T	p.(Gln361*)	Y	612034	stop_gained	HIGH	NM_005883.2		0.000000	-	-	36	
Family 2	AMY2A	hom	1	104160661	G	A	c.254G>A	p.(Cys85Tyr)		104650	missense_variant	MODERATE	NM_000699.3		-	tolerated(0.2)	probably_damagi	17.93	
	EPHA5	hom	4	66231748	A	C	c.1952T>G	p.(Ile651Ser)		600004	missense_variant	MODERATE	NM_004439.7		-	deleterious(0.02)	possibly_damagin	24.7	
	HOXC10	hom	12	54379276	C	T	c.233C>T	p.(Ser78Phe)		605560	missense_variant	MODERATE	NM_017409.3		-	deleterious(0.01)	benign(0.276)	25.9	
	BRCA2	hom	13	32905126	C	G	c.752C>G	p.(Thr251Arg)		600185	missense_variant	MODERATE	NM_000059.3	587781513	0.000004	tolerated(0.18)	probably_damagi	7.681	Fanconi anemia (MIM 605724)
	CDC42BPB	hom	14	103410287	G	A	c.4349C>T	p.(Pro1450Leu)		614062	missense_variant	MODERATE	NM_006035.3		0.000016	tolerated(0.76)	benign(0.003)	17.13	
	APC2	hom	19	1465182	C	T	c.1882C>T	p.(Gln628*)	Y	612034	stop_gained	HIGH	NM_005883.2		-	-	-	40	
	DEPDC5	hom	22	32188752	G	A	c.716G>A	p.(Arg239Gln)		614191	missense_variant	MODERATE	NM_001007188		0.000010	deleterious(0.03)	possibly_damagin	25.3	
Family 3	MIDN	hom	19	1255457	G	A	c.893G>A	p.(Arg298Gln)		606700	missense_variant	MODERATE	NM_177401.4	143719550	0.000295	deleterious(0)	possibly_damagin	23.5	
	APC2	hom	19	1469940	C	-	c.6645delC	p.(Ala2217Profs*118)	Y	612034	frameshift_variar	HIGH	NM_005883.2		-	-	-	-	
Family 4	SPEG	hom	2	220348409	T	G	c.6224T>G	p.(Leu2075Arg)		615950	missense_variant	MODERATE	NM_005876.4	892492321	0.000016	deleterious(0)	probably_damagi	24.3	Centronuclear myopathy 5 (MIM 615959)
	UGT2B17	hom	4	69416566	A	T	c.1142T>A	p.(Ile381Asn)		601903	missense_variant	MODERATE	NM_001077.3	749202776	0.000020	deleterious(0)	probably_damagi	26.3	
	ZFHX4	hom	8	77618200	G	A	c.1877G>A	p.(p.Arg626Lys)		606940	missense_variant	MODERATE	NM_024721.4	751323188	0.000032	deleterious(0.03)	possibly_damagin	14.46	
	FGF6	hom	12	4554487	G	A	c.250C>T	p.(Arg84Trp)		134921	missense_variant	MODERATE	NM_020996.1	373061794	0.000040	deleterious(0.02)	possibly_damagin	25	
	SERPINF1	hom	17	1675327	G	C	c.601G>C	p.(Asp201His)		172860	missense_variant	MODERATE	NM_001329903.1	137997656	0.000008	tolerated(0.17)	benign(0.404)	6.925	Osteogenesis imperfecta, type VI (MIM 613982)
	SMYD4	hom	17	1703330	T	-	c.1358delA	p.(Gln453Argfs*2)			frameshift deletic	HIGH	NM_052928.2	755710047	0.000096	-	-	32	
	APC2	hom	19	1462016	CA	-	c.1694_1695delCA	p.(Thr565Argfs*50)	Y	612034	frameshift deletic	HIGH	NM_005883.2	.	-	-	-	-	
	ATP4A	hom	19	36046673	G	-	c.1911delC	p.(Ile638Leufs*26)		137216	frameshift deletic	HIGH	NM_000704.2	.	-	-	-	-	
	AX746638	hom	19	36806475	A	T	c.143T>A	p.(Leu48Gln)			missense_variant	MODERATE	NR_029389.1	2967481	-	-	-	-	
	SRRM5;ZNF5	hom	19	44116719	G	A	c.491G>A	p.(Gly164Asp)			missense_variant	MODERATE	NM_001145641.1	.	-	deleterious(0.04)	possibly_damagin	22.8	
	MARK4	hom	19	45790731	C	T	c.1303C>T	p.(Pro435Ser)		606495	missense_variant	MODERATE	NM_001199867.1	.	-	tolerated(0.16)	benign(0.3)	24.6	
	RPL18	hom	19	49121116	T	C	c.22A>G	p.(Asn8Asp)		604179	missense_variant	MODERATE	NM_000979.3	.	-	tolerated(0.25)	benign(0.014)	19.96	
	NTN5	hom	19	49165133	T	C	c.1271A>G	p.(Gln424Arg)			missense_variant	MODERATE	NM_145807.1	760927020	0.000133	tolerated(1)	benign(0.003)	0.001	
	LRRC4B	hom	19	51051969	C	T	c.127G>A	p.(Val43Met)			missense_variant	MODERATE	NM_001080457.1	753942999	0.000236	tolerated(0.07)	benign(0.005)	23.2	
	RIMBP3C	hom	22	21900617	A	G	c.4649T>C	p.(Ile1550Thr)		612701	missense_variant	MODERATE	NM_001128633.1	484252	-	tolerated(1)	benign(0)	0.001	
Family 8	IGSF9	hom	1	159899764	T	A	c.2066A>T	p.Asp689Val		609738	missense_variant	MODERATE	NM_001135050.1	201810988	0.000300	deleterious	probably_damagi	26.5	
	MEGF6	hom	1	3418428	G	A	c.2246C>T	p.Ala749Val		604266	missense_variant	MODERATE	NM_001409.3	200472001	0.001700	tolerated	probably_damagi	22.5	
	HS1BP3	hom	2	20840790	G	A	c.349C>T	p.Arg117Cys		609359	missense_variant	MODERATE	NM_022460.3	377728516	0.000050	deleterious	probably_damagi	29.7	
	CDHR4	hom	3	49834383	G	A	c.578C>T	p.Ser193Phe			missense_variant	MODERATE	NM_001007540.3	560357842	0.00009	-	probably_damagi	24.7	
	LAMB2	hom	3	49160696	G	A	c.4093C>T	p.Arg1365Trp		150325	missense_variant	MODERATE	NM_002292.3	751854328	0.0002	deleterious	probably_damagi	26.3	Nephrotic syndrome, type 5, with or without ocular abnormalities (MIM 614199), Pierson syndrome (MIM 609049)
	SEMA3B	hom	3	50311438	C	A	c.1086C>A	p.His363Asn		601281	missense_variant	MODERATE	NM_004636.3	782238556	0.000060	deleterious	-	20.5	
	TREX1	hom	3	48508733	G	A	c.679G>A	p.Gly227Ser		606609	missense_variant	MODERATE	NM_033629.5	113107733	0.0002	tolerated	-	15.7	Aicardi-Goutieres syndrome 1, dominant and recessive (MIM 225750)
	ULK4	hom	3	41291010	C	T	c.3734G>A	p.Arg1245Gln		617010	missense_variant	MODERATE	NM_017886.3	756001134	0.00002	tolerated	benign	<10	
	FILIP1	hom	6	76063397	G	A	c.487C>T	p.Arg163Trp		607307	missense_variant	MODERATE	NM_015687.4	759270192	0.0001	deleterious	probably_damagi	28.4	
	GABRR2	hom	6	89974256	C	T	c.961G>A	p.Val321Ile		137162	missense_variant	MODERATE	NM_002043.4	2228644	-	tolerated	-	15	
	TAS2R60	hom	7	143141342	G	C	c.797G>C	p.Ser266Thr		613968	missense_variant	MODERATE	NM_177437.1	-	-	tolerated	benign	<10	
	CSMD1	hom	8	3611478	C	T	c.905G>A	p.Arg302His		608397	missense_variant	MODERATE	NM_033225.5	754405745	0.00002	-	probably_damagi	23.9	
	FAM189A1	hom	15	29415846	C	T	c.1316G>A	p.Arg439His			missense_variant	MODERATE	NM_015307.1	61736883	0.000500	tolerated	benign	14.6	
	HERC2	hom	15	28467280	T	C	c.5546A>G	p.Lys1849Arg		605837	missense_variant	MODERATE	NM_004667.5	201821203	0.00057233	-	benign	17.1	Mental retardation, autosomal recessive 38 (MIM 615516)
	FSCN2	hom	17	79503213	G	A	c.1025G>A	p.Arg342Gln		607643	missense_variant	MODERATE	NM_001077182.2	374441539	0.000090	tolerated	benign	23.6	
	MAPRE2	hom	18	32558480..32558483	GAA	-	c.-2_2delGAAT	p.Met1		605789	initiation_codon	HIGH	NM_001143827.2	764635254	0.0015	-	-	22.1	
	APC2	hom	19	1462177	G	C	c.1853+1G>C		Y	612034	splice site disrupt	HIGH	NM_005883.2	-	-	-	-	32	

Table S1. High impact homozygous variants returned from whole exome sequencing of Families 1-4. In each family, a homozygous damaging mutation in *APC2* was determined to be most likely causative based upon objective filtering criteria (yellow).

Supplemental Methods

Study samples

We performed whole exome sequencing (WES) in 8 families with affected(s) displaying features consistent with lissencephaly, where prior gene panels and microarray studies proved negative at identifying a cause of disease. Subjects were enrolled in IRB-approved research studies at the University of California, San Diego or their home institution (Institute for Clinical Genetics, TU Dresden, Germany, University of Washington, National Research Center Egypt, St. George's University of London, Erasmus University, Istanbul University, The George Washington University and Mashhad University).

Exome sequencing and variant calling

Blood was acquired from informed, consenting individuals or their surrogates, according to institutional guidelines, and DNA extracted using established protocols. In solution exome capture was preformed using the SureSelect Human All Exome 50 Mb Kit (Agilent Technologies, USA) or xGen exome research panel (Integrated DNA Technologies, USA) with 100- or 150-bp paired-end read sequences generated on a HiSeq4000 or NextSeq500 instruments (Illumina, Inc. USA). Sequences were aligned to hg19 and variants identified through the GATK pipeline or CLC Biomedical Genomics Workbench (Qiagen, Hilden, Germany). Variations were annotated with in-house software, Annovar, Variant Effect Prediction software or CLC Biomedical Genomics Workbench to define population-specific allele frequencies from 1000 Genomes, the Greater Middle East Variome, dbSNP, and gnomAD, along with the transcript-specific predicted effect on the protein. All variants were prioritized by allele frequency, conservation, and predicted effect on protein function.

Variant prioritization

Variants were prioritized for each family using the following criteria:

1. The variant was predicted to perturb protein function. All synonymous and intronic variants were excluded unless the variant was within a predicted splice site (+ or -2 bp from splice junction). Any variation that was predicted to alter gene expression or protein function was included. These included nonsynonymous variations in coding regions (i.e. missense) or

alterations resulting in frameshifts, premature stop codons, loss of stop codons, coding INDELS, and splice sites (i.e. ±2 nucleotides from an exon junction).

2. The variant was rare as defined by allele frequency of less than 0.1% in either gnomAD or GME variomes.

3. The variant was present in a region of homozygosity as defined by HomozygosityMapper or parametric linkage analysis for consanguineous families.

4. The variant was conserved evolutionary as determined by a number of conservation scores including GERP, PhastCons, and PolyPhen2. Variations with negative GERP scores or vertebrate PhastCons scores less than 0.8 were excluded. Typical conservation criteria for the candidate genes provided in this study were GERP > 4 and vertebrate PhastCons > 0.9.

5. The variant was confirmed using Sanger sequencing and segregated with the disease in the family pedigree according to a strictly recessive mode of inheritance with full expressivity and absent phenotype in heterozygous carriers.

All variants following the above criteria were considered for each family independent of its predicted severity (i.e. no variants were excluded based upon type of mutation).

Sanger sequencing

Primers for Sanger sequencing were designed using the Primer3 program (U. Massachusetts) and tested for specificity using the Alamut Visual 2.7.1 software. PCR products were treated with Exonuclease I (Fermentas) and Shrimp Alkaline Phosphatase (USB Corp) and sequenced using the Big Dye terminator cycle sequencing kit v.3.1 (Applied Biosystems) on an ABI DNA analyzer (Applied Biosystems). Sequence data were analyzed using ApE1® software.